

Mahdi S. Edan

Department of Quality Assurance,
Ministry of Higher Education and
Scientific Research,
Baghdad, IRAQ
Corresponding author:
mahdiedan@yahoo.com



Structural and Optoelectronic Characteristics of Nanostructured Multilayer CuO/ZnO Heterojunction for UV and Visible Laser Photodetectors

In this work, the dc reactive sputtering technique was used to fabricate multilayer structures from nanostructured copper oxide (CuO) and zinc oxide (ZnO) thin films on indium-doped tin dioxide (ITO) substrates. The structural and morphological characteristics of these samples were introduced by the X-ray diffraction (XRD), field-emission scanning electron microscopy (FE-SEM), and atomic force microscopy (AFM). As well, the spectral responsivity and external quantum efficiency (EQE) of the fabricated heterojunction were determined to show their feasibility as multi-wavelength photodetectors. The optimum heterojunction configured from a 200nm-thick CuO layer deposited on a 200nm-thick ZnO layer deposited on ITO substrate showed maximum responsivity of 0.83 and 0.59 A/W at 347 and 585 nm, respectively. Also, it showed maximum EQE of 1.45 and 0.62 at 347 and 585 nm, respectively. This device exhibits high reliability, reasonable efficiency, high reproducibility, and low production cost with good control on fabrication parameters.

Keyword: Heterojunctions; Laser photodetectors; Zinc oxide; Copper oxide

Received: 20 July 2025; Revised: 16 September 2025; Accepted: 23 September; Published: 1 April 2026

1. Introduction

Development of optoelectronic devices with high performance, low production cost, high reliability and good reproducibility has driven intensive research works into semiconducting multilayer thin film heterojunctions. Such devices are engineered by sequentially deposition of two or more dissimilar metal oxide layers to create a vital interfacial region where their distinct electronic properties interact [1-3]. Physical vapor deposition (PVD) methods and techniques, such as magnetron sputtering, pulsed-laser deposition, ion beam deposition, provide precise control over film stoichiometry, layer thickness, interfacial quality and nanostructural morphology [4,5]. Such control is essential since the structural and electronic characteristics of the interface formed within the heterojunction structure directly determines the ultimate performance of the device [6-8].

Amongst semiconducting metal oxides, ZnO and CuO and their devices have emerged a particularly promising platform to develop low-cost efficient photonics and optoelectronics. The fabrication and characterization of CuO/ZnO heterojunctions is motivated by a confluence of inherent material advantages. Copper oxide (CuO) is a p-type semiconductor with a narrow energy band gap (1.2-1.7 eV), which provides efficient absorption in the visible region of electromagnetic spectrum [9,10]. Zinc oxide (ZnO) is an n-type semiconductor with wide energy band gap (3.2-3.3 eV), which shows high electron mobility, high transparency, and strong excitonic binding energy [11,12]. The CuO/ZnO heterojunction forms a type-II band alignment that facilitates the effective spatial separation of the photo-generated

electron-hole pairs across the junction. This charge separation is a main advantage as it drastically reduces the recombination losses and enhances the quantum efficiency of the optoelectronic processes [13-15]. Moreover, ZnO and CuO are composed of abundant, non-toxic elements, and offer robust chemical and thermal stabilities. Also, they are compatible with large-area, low-temperature fabrication processes [16,17]. These materials also show good ability to tailor their nanostructures into nanorods, nanowires, or granular films, which support their functionality by increasing the interfacial surface area and introducing light-trapping or quantum confinement effects [18-20].

The CuO/ZnO heterojunctions are ideal choice to construct self-powered, broadband photodetectors that respond to a wide spectrum extending from UV to near infrared (NIR) with fast response, high gain, and low noise level [21-23]. These features make them suitable for optical communications and environmental sensing. These heterojunctions represent the basement for the third-generation photovoltaic devices, including dye-sensitized and perovskite solar cells as they are successfully used as efficient electron-transport layers and hole-blocking contacts [24,25]. These heterojunctions are employed in photocatalytic systems for environmental remediation and hydrogen generation [26,27]. They were explored for light-emitting diodes (LEDs) and thin film transistors (TFTs) [28,29].

On the other hand, the optimum performance of such heterojunctions is reasonably determined by the precise manipulation of their structural and optoelectronic characteristics at the nanoscale. Parameters, like the crystallinity, phase purity, defect

density, and the abruptness of the heterojunction interface, are critical in determining the fabrication method. Therefore, a deposition method with high ability to control preparation conditions, such as dc reactive magnetron sputtering, is the solution.

The aim of this research is to fabricate multilayer nanostructured thin film CuO/ZnO heterojunctions and introduce their structural, morphological and optoelectronic characteristics.

2. Experimental work

A homemade dc reactive magnetron sputtering system was used to deposit ZnO and CuO thin films on ITO substrates. The Zn target – then Cu target – was cleaned, dried and maintained carefully on the cathode to start the deposition process in presence of oxygen gas as a reactive gas. The ITO substrates were initially cleaned before the deposition experiments. The plasma required for sputtering was generated by the electric discharge of argon. Electrical power was provided by a high-voltage DC power supply. The operating conditions of the system include initial vacuum pressure of 0.01 mbar, discharge voltage of 1-1.5 kV, discharge current of 20-30 mA, Ar:O₂ gas mixing ratio of 50:50, gas mixture flow rate of 15 sccm, and inter-electrode distance of 4 cm. deposition time was selected to be 90 minutes according to optimization in previous works on the same system [30-33]. Film thickness was measured by laser interferometry method to be 200 nm for individual layers and figure (1) shows schematically the design of the CuO/ZnO structure fabricated in this work.

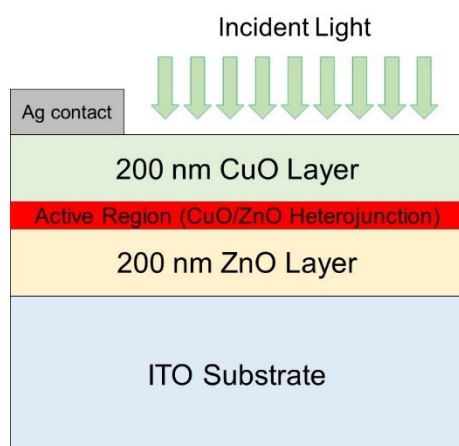


Fig. (1) Schematic diagram of the CuO/ZnO heterostructure fabricated in this work

The structural characteristics of the extracted nanopowders were determined by x-ray diffraction (XRD), field-emission scanning electron microscopy (FE-SEM), and atomic force microscopy (AFM). The optical characteristics were introduced using a UV-visible spectrophotometer, while the electrical characteristics were determined using a DC power

supply, digital ammeter, and irradiation source (halogen lamp). Also, two laser diodes (380 nm and 530 nm) were used to examine the spectral responsivity of the fabricated heterojunctions as laser photodetectors.

3. Results and Discussion

Figure (2) shows the XRD patterns of the CuO and ZnO thin films prepared in this work. These patterns reveal distinct polycrystalline phases for CuO and ZnO films that confirm the successful deposition by dc reactive magnetron sputtering technique. The CuO film shows monoclinic phase with sharp, intense peaks at 32.51°, 35.53°, 38.71°, 48.71°, 53.45°, 58.46°, 61.51°, 66.23°, 68.10°, 72.62°, and 75.23° according to the JCPDS card 96-901-6327. The average crystallite size is about 37 nm. The ZnO film exhibits characteristic diffraction peaks at 31.91°, 34.51°, 36.38°, 47.71°, 56.65°, 63.09°, 68.00°, and 69.23°, with three additional weak peaks at 66.53°, 72.64°, and 77.05°. These collections of diffraction peaks correspond to the hexagonal wurtzite structure of ZnO according to the JCPDS cards 96-901-1663 and 96-153-8018. The average crystallite size according to Scherrer's formula is about 46 nm. Both materials show good crystallinity, which is essential for the charge transport in the CuO/ZnO heterojunction to be efficient. As no significant impurity peaks were seen, the phase-pure film formation is revealed. The interfacial properties and overall performance of the fabricated heterojunction can be optimized by the structural quality of the heterojunction [34,35].

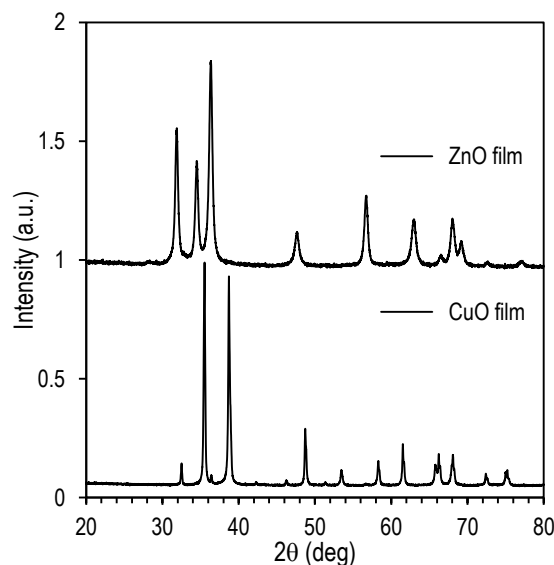


Fig. (2) XRD patterns of CuO and ZnO thin films prepared in this work

Figure (3) shows the FE-SEM images of the CuO and ZnO film samples prepared in this work. They show uniform, well-defined nanostructures. Moreover, the ZnO sample exhibits a dense, finely grained morphology with minimum particle size of about 15

nm, while the CuO sample exhibits slightly much more granular clustering with minimum particle size of about 20 nm. The prepared nanostructures are advantageous for the fabrication of CuO/ZnO heterojunctions as the uniform surfaces ensure intimate interfacial contact, which is essential for efficient charge transfer in optoelectronics and photovoltaic devices. As well, distinct and compatible morphologies allow an effective layer-by-layer integration that enables the formation of a p-n junction with minimum defects, and hence enhanced device performance in sensors and solar cells [35,36].

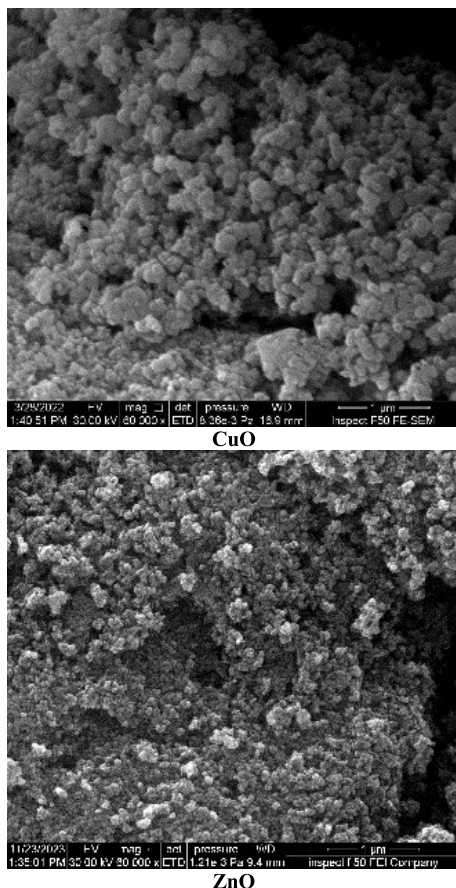


Fig. (3) FE-SEM images of CuO and ZnO thin films prepared in this work

Figure (4) shows the 3D AFM images for both film samples (CuO and ZnO) prepared in this work. These images provide detailed surface topography of both samples revealing significant differences in their nanostructures. The ZnO film shows relatively dense, uniform morphology with moderate surface roughness with average grain size of 40-50 nm. This suggests continuous layer formation. On the other hand, the CuO film exhibits much more granular topography with larger, distinct grain-like features and higher surface roughness with average grain size of 80-100 nm. This indicates a porous, agglomerated nanostructure.

The combination of these two layers is highly advantageous to fabricate high-quality heterojunction as the smooth, compact ZnO layer provides excellent electron-transport pathway and uniform interface, whereas the rougher CuO layer enhances light trapping and charge separation. This synergetic effect is exceptionally beneficial for optoelectronics such as photodetectors and solar cells where efficient charge collection and broad spectral absorption are essential [36,37].

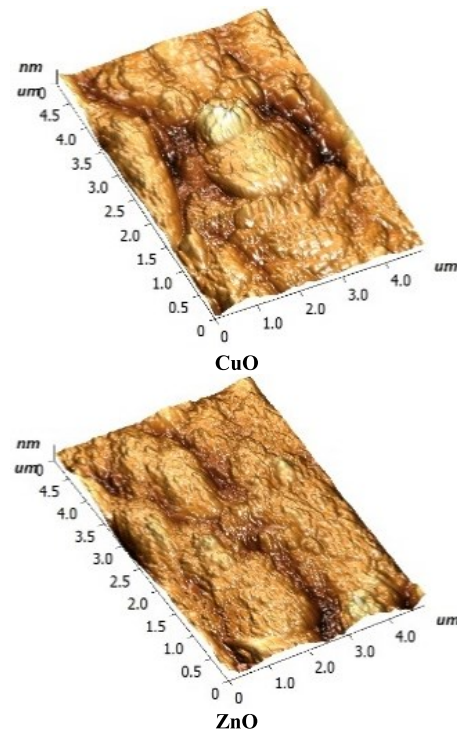


Fig. (4) 3D AFM images of CuO and ZnO thin films prepared in this work

Figure (5) shows the absorption spectra of the CuO, ZnO, and CuO/ZnO thin film samples prepared in this work. These spectra reveal significant insights into the optical properties and electronic interactions within these materials. The absorption spectrum of ZnO (black line) shows a characteristic sharp absorption onset in the UV region around 375-400 nm. This edge corresponds to the intrinsic energy band gap of ZnO (3.2-3.3 eV). The absorption rises at shorter wavelengths due to the excitation of electrons from the valence band to the conduction band. In the visible and near-infrared (NIR) regions, the ZnO film shows very low absorbance (approximately transparent), which is a property for transparent conductive oxide (TCO) such as ZnO.

The CuO film spectrum is markedly different from that of ZnO as a strong, broad absorption is observed across the visible and NIR regions. Much more gradual absorption onset can be seen around 600-700 nm extending beyond 1000 nm. This reveals the narrower band gap of CuO (1.2-1.7 eV), which enables it to

respond to the visible light. The absorption tail indicates the indirect transitions within the band gap, possible defect states, or sub-band absorption, due to much more complex electronic structure compared to ZnO [37,38].

The absorption spectrum of CuO/ZnO structure shows a behavior between the spectra of CuO and ZnO individually. In the UV region, it follows the absorption edge of ZnO and confirms the presence of ZnO layer. Within the range 400-800 nm, the structure shows higher absorbance than that of ZnO film, but still lower than that of CuO. This enhancement is attributed to one or more of three interfacial phenomena: improved light trapping within the layered structure, reduced reflectance due to graded refractive indices, or formation of a type-II (staggered) heterojunction at the CuO/ZnO interface, at which the conduction and valence band offsets facilitate the spatial separation of photo-generated electrons and holes migrating to both sides of the structure. This suppresses the recombination and potentially leads increase effective photon absorption.

Moreover, the spectrum of CuO/ZnO structure as a mirror of CuO spectrum extended into the NIR region confirms the ability of this structure to harness a broader solar spectrum. This design combining wide and narrow bandgap semiconducting materials represents the principle behind many advanced heterojunction photodetectors and tandem photovoltaic cells [6,13,17,24,25].

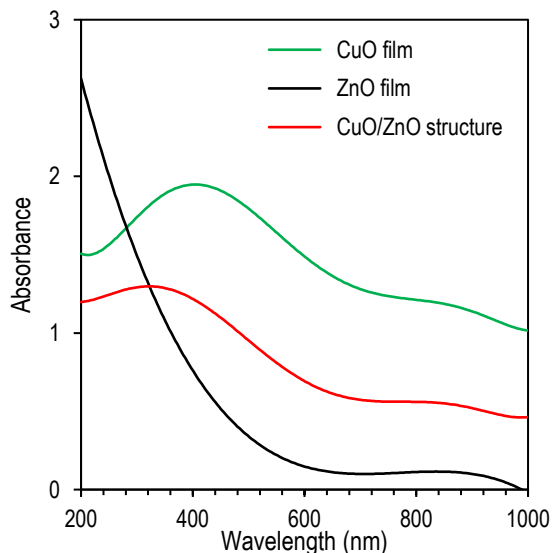


Fig. (5) Absorption spectra of CuO film, ZnO film, and 200nm-CuO/200nm-ZnO structure

Figure (6) shows the spectral responsivity (R_s) of the nanostructured multilayer CuO/ZnO thin film heterostructure prepared in this work in the spectral range of 300-800 nm. This figure exhibits a pronounced, broad response peak in the UV region (at 347 nm) with maximum responsivity of 0.83 A/W. This

peak aligns with the fundamental absorption edge of ZnO, indicating that the wide-bandgap layer (ZnO) is the primary photoactive material in this spectral range. The high responsivity reveals the efficient carrier generation and collection upon UV photon absorption, which is enhanced by the multilayer nanostructures due to increasing surface area and light-trapping within the ZnO layer. Another peak seen at 585 nm with responsivity up to 0.6 A/W aligns with the high absorbance of CuO layer as a narrow bandgap material.

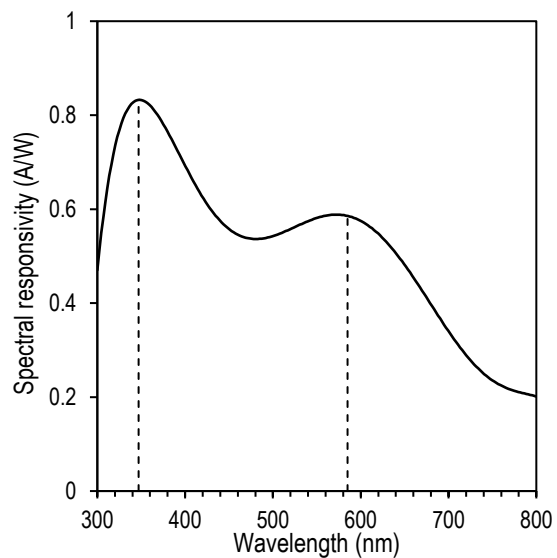


Fig. (6) Spectral responsivity of the nanostructured multilayer 200nm-CuO/200nm-ZnO/ITO heterostructure prepared in this work

At wavelengths longer than 585 nm, the responsivity gradually decreases to a minimum of 0.2 A/W within 750-800 nm. This behavior corresponds to the decreasing photon energy, which eventually falls below the effective optical gap of the CuO/ZnO system. The persistent response suggests the effective operation of such type-II heterojunction, in which the photo-excited electrons in CuO layer can transfer to the conduction band of ZnO, while the holes move in the opposite direction, facilitating charge separation and reducing recombination. This interfacial charge transfer mechanism allows the heterostructure to harvest a wider range of photons than each material can individually.

Similarly, the behavior of the external quantum efficiency (EQE) shown in Fig. (7) strongly correlates with the spectral responsivity discussed before. A significant peak at 347 nm with maximum value of 1.45% is attributed to the strong absorption and efficient charge charge collection from the ZnO layer. The EQE then decreases gradually across the visible region but remains measurable out to ~700 nm, which confirms the broadband response of the heterostructure. Obviously, this extended response is enabled by the CuO absorption and effective charge separation at the

heterojunction interface, where the photo-generated charge carriers are efficiently collected despite the lower photon energies.

4. Conclusions

In concluding remarks, the nanostructured multilayer CuO/ZnO heterojunction was successfully fabricated by dc reactive magnetron sputtering technique. The optoelectronic characteristics of the fabricated heterojunction showed a dual-peak spectral responsivity (0.83 A/W at 347 nm and 0.59 A/W at 585 nm) and corresponding external quantum efficiency, confirming effective broadband detection from UV to visible light. These results highlight the potential of the CuO/ZnO heterostructure device for practical applications in sensing, communications, and solar energy conversion.

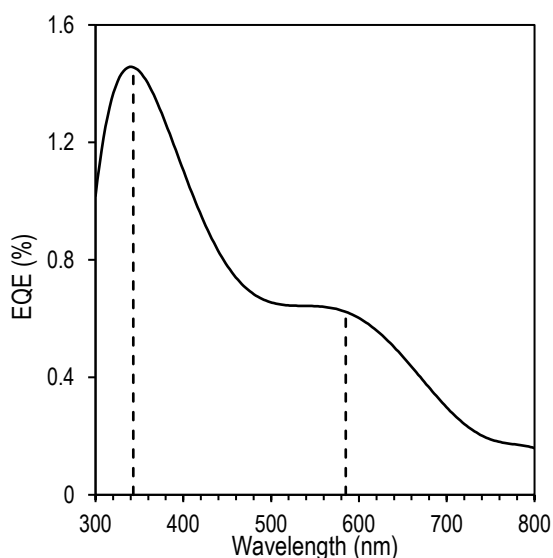


Fig. (7) External quantum efficiency (EQE) of the nanostructured multilayer 200nm-CuO/200nm-ZnO/ITO heterostructure prepared in this work

References

[1] G. Li et al., "Enhanced chemiresistive sensing performance of well-defined porous CuO-doped ZnO nanobelts toward VOCs", *Nanoscale Adv.*, 1(10) (2019) 3900-3908.

[2] O.A. Hamadi, "Profiling of Antimony Diffusivity in Silicon Substrates using Laser-Induced Diffusion Technique", *Iraqi J. Appl. Phys. Lett.*, 3(1) (2010) 23-26.

[3] H. Sadiq et al., "Preparation and photocatalytic degradation of ZnO/Fe₃O₄/GO heterojunction via synergistic electron-hole separation", *Mater. Sci. Eng. B*, 324(A) (2026) 118903.

[4] J.A. Yaseen, "Effects of Silicon Dioxide Layer on Optoelectronic Characteristics of FeO/PSi Heterostructures", *Iraqi J. Appl. Phys. Lett.*, 8(4) (2025) 99-102.

[5] J.W. Yang et al., "Nanoporous oxide electrodes for energy conversion and storage devices", *RSC Appl. Interfaces*, 1(1) (2024) 11-42.

[6] K.A. Jagadish and D. Kekuda, "Performance analysis of a DC magnetron sputtered Cu₂O/TiO₂ heterojunction photodetector for short-wavelength detection", *Sens. Actuat. A: Phys.*, 388 (2025) 116517.

[7] L. Wang et al., "Progress and perspectives of self-powered gas sensors", *Next Mater.*, 2 (2024) 100092.

[8] M. Coll et al., "Towards Oxide Electronics: a Roadmap", *Appl. Surf. Sci.*, 482 (2019) 1-93.

[9] M. Lu et al., "Cu₂O/Co₃O₄ nanoarrays for rapid quantitative analysis of hydrogen sulfide in blood", *Nanoscale Adv.*, 5(6) (2023) 1784-1794.

[10] M.A. Ahmed, S.A. Mahmoud and A.A. Mohamed, "Unveiling the photocatalytic potential of graphitic carbon nitride (g-C₃N₄): a state-of-the-art review", *RSC Adv.*, 14(35) (2024) 25629-25662.

[11] M.K. Verma et al., "Core-shell nanoparticles for water purification: Advances in photocatalytic and antimicrobial applications", *Next Mater.*, 9 (2025) 101186.

[12] M.M. Ahmed and R.S. Behnam, "Sheet Resistance of Cobalt/Silicon Ohmic Contacts Fabricated by Laser-Induced Diffusion", *Iraqi J. Appl. Phys. Lett.*, 7(4) (2024) 3-5.

[13] J.A. Yaseen, "Influence of FeO Layer Thickness on Characteristics of FeO/Porous Silicon Heterojunction Photodetectors", *Iraqi J. Mater.*, 4(4) (2025) 153-162.

[14] M.-Y. Dai et al., "First-principles calculations of the photocatalytic performance of ZnO-MX₂ (M = Mo, W; X = S, Se) heterojunctions", *RSC Adv.*, 15(29) (2025) 23489-23498.

[15] N. Alomayrah et al., "Fabrication of a highly efficient CuO/ZnCo₂O₄/CNTs ternary composite for photocatalytic degradation of hazardous pollutants", *RSC Adv.*, 14(34) (2024) 24874-24897.

[16] N. Zhang et al., "Research progress on nanomaterial-empowered electrochemical biosensors for the detection of cardiac troponin I", *RSC Adv.*, 15(32) (2025) 26473-26489.

[17] N.A.H. Hashim and T.A. Almashhadani, "Optoelectronic Characteristics of Co₃O₄ NPs/PSi/Si Photodetector", *Iraqi J. Appl. Phys. Lett.*, 9(1) (2026) 34-37.

[18] N.A.H. Hashim, F.J. Kadhim and Z.S. Abdulsattar, "Characterization of Electrochromism and Photoelectrochromism of N-Doped TiO₂ and Co₃O₄ Thin Films Prepared by DC Reactive Magnetron Sputtering: Comparative Study", *Iraqi J. Appl. Phys.*, 19(1) (2023) 5-12.

[19] N.M. Hieu et al., "ZnTe-coated ZnO nanorods: Hydrogen sulfide nano-sensor purely controlled by pn junction", *Mater. Design*, 191 (2020) 108628.

- [20] O.A. Hammadi, F.J. Kadhim and E.A. Al-Oubidy, "Photocatalytic Activity of Nitrogen-Doped Titanium Dioxide Nanostructures Synthesized by DC Reactive Magnetron Sputtering Technique", *Nonl. Opt. Quantum Opt.*, 51(1-2) (2019) 67-78.
- [21] Q.F. Sadoon, M.S. Jassem and A.J. Nasori, "Morphological Characteristics of Plasma-Etched Silicon Substrates Coated with Nickel Oxide Nanoparticles for Optoelectronics Applications", *Iraqi J. Appl. Phys. Lett.*, 7(4) (2024) 6-8.
- [22] R.K. Paul and Md. Ahmaruzzaman, "Advanced photocatalytic degradation of POPs and other contaminants: a comprehensive review on nanocomposites and heterojunctions", *RSC Adv.*, 15(38) (2025) 31313-31359.
- [23] R.N. Khoshnaw, "Characteristics of CoO/Si Heterostructure Prepared by Plasma-Induced Bonding", *Iraqi J. Appl. Phys. Lett.*, 7(2) (2024) 19-22.
- [24] S. Tahiri, "Heterojunction Solar Cell Based on Highly-Pure Nanopowders Prepared by DC Reactive Sputtering Technique", *Iraqi J. Mater.*, 3(2) (2024) 77-82.
- [25] S.H. Faisal and M.A. Hameed, "Heterojunction Solar Cell Based on Highly-Pure Nanopowders Prepared by DC Reactive Magnetron Sputtering", *Iraqi J. Appl. Phys.*, 16(3) (2020) 27-32.
- [26] S.K. Srivastava, "Recent advances in removal of pharmaceutical pollutants in wastewater using metal oxides and carbonaceous materials as photocatalysts: a review", *RSC Appl. Interface.*, 1(3) (2024) 340-429.
- [27] V. Paolucci et al., "SnO₂ quantum dot decoration of CuO nanoparticles with enhanced NO₂ and H₂ gas sensing response via p-n heterojunction interfaces", *RSC Adv.*, 15(46) (2025) 38750-38761.
- [28] V.S. Ghodake et al., "Exploring the antibacterial properties of ZnO nanorods-CuO nanoflowers: a mode of action approach", *RSC Adv.*, 15(40) (2025) 32995-33005.
- [29] A.M. Hameed and M.A. Hameed, "Highly-Pure Nanostructured Metal Oxide Multilayer Structure Prepared by DC Reactive Magnetron Sputtering Technique", *Iraqi J. Appl. Phys.*, 18(4) (2022) 9-14.
- [30] A.M. Hameed and M.A. Hameed, "Spectroscopic characteristics of highly pure metal oxide nanostructures prepared by DC reactive magnetron sputtering technique", *Emergent Materials*, 6 (2022) 627-633.
- [31] F.J. Al-Maliki and E.A. Al-Oubidy, "Effect of gas mixing ratio on structural characteristics of titanium dioxide nanostructures synthesized by DC reactive magnetron sputtering", *Physica B: Cond. Matter*, 555 (2019) 18-20.
- [32] N.A.H. Hashim and F.J. Kadhim, "Structural and Optical Characteristics of Co₃O₄ Nanostructures Prepared by DC Reactive Magnetron Sputtering", *Iraqi J. Appl. Phys.*, 18(4) (2022) 31-36.
- [33] R.H. Turki and M.A. Hameed, "Spectral and Electrical Characteristics of Nanostructured NiO/TiO₂ Heterojunction Fabricated by DC Reactive Magnetron Sputtering", *Iraqi J. Appl. Phys.*, 16(3) (2020) 39-42.
- [34] M.A. Hameed, S.H. Faisal, R.H. Turki, "Characterization of Multilayer Highly-Pure Metal Oxide Structures Prepared by DC Reactive Magnetron Sputtering Technique", *Iraqi J. Appl. Phys.*, 16(4) (2020) 25-30.
- [35] R.H. Turki and M.A. Hameed, "Spectral and Electrical Characteristics of Nanostructured NiO/TiO₂ Heterojunction Fabricated by DC Reactive Magnetron Sputtering", *Iraqi J. Mater.*, 3(3) (2024) 39-44.
- [36] A.S. Falah and K.R. Jasim, "Simulation Study on Current Gain Improvement at High Collector Current Densities for CuO/TiO₂ Heterostructure Transistors", *Iraqi J. Mater.*, 3(4) (2024) 25-30.